MOLECULAR AND CELLULAR BIOLOGY, July 2005, p. 5579–5589 Vol. 25, No. 13
0270-7306/05/$08.00+0 doi:10.1128/MCB.25.13.5579–5589.2005

Dimerization of CUL7 and PARC Is Not Required for All CUL7 Functions and Mouse Development

Jeffrey R. Skaar, Takehiro Arai,† and James A. DeCaprio*

Dana-Farber Cancer Institute, Department of Medical Oncology, and Harvard Medical School, Boston, Massachusetts

Received 25 January 2005/Returned for modification 28 January 2005/Accepted 8 April 2005

CUL7, a recently identified member of the cullin family of E3 ubiquitin ligases, forms a unique SCF-like complex and is required for mouse embryonic development. To further investigate CUL7 function, we sought to identify CUL7 binding proteins. The p53-associated, parkin-like cytoplasmic protein (PARC), a homolog of CUL7, was identified as a CUL7-interacting protein by mass spectrometry. The heterodimerization of PARC and CUL7, as well as homodimerization of PARC and CUL7, was confirmed in vivo. To determine the biological role of PARC by itself and in conjunction with CUL7, a targeted deletion of *Parc* was created in the mouse. In contrast to the neonatal lethality of the *Cul7* knockout mice, *Parc* knockout mice were born at the expected Mendelian ratios and exhibited no apparent phenotype. Additionally, *Parc* deletion did not appear to affect the stability or function of p53. These results suggest that PARC and CUL7 form an endogenous complex and that PARC and CUL7 functions are at least partially nonoverlapping. In addition, although PARC and p53 form a complex, the absence of effect of *Parc* deletion on p53 stability, localization, and function suggests that p53 binding to PARC may serve to control PARC function.

The ubiquitin-proteasome system plays an important role in controlling diverse biological processes, ranging from signal transduction to cell cycle control. The covalent addition of ubiquitin to proteins is the result of a sequential cascade in which ubiquitin is activated by the E1 ubiquitin-activating enzyme, transferred to an E2 ubiquitin-conjugating enzyme, and transferred to a lysine residue on the substrate by an E3 ubiquitin ligase (10). Reiteration of this cascade leads to the formation of a polyubiquitin chain, targeting the substrate to the proteasome for degradation.

The substrate specificity, and thus ultimate control of the ubiquitination reaction, is determined by the E3 ubiquitin ligase. Many E3 ligase complexes have been identified, and they are generally grouped into two categories based on the presence of either a HECT domain protein or a RING protein in the complex. The canonical SCF (SKP1/CUL1/F-box) complex is a prototype RING-type E3 ligase, with the core cullin scaffold recruiting the small RING protein RBX1 in addition to SKP1 and a variable F-box (3, 5). In this complex, RBX1 recruits the E2 enzyme and SKP1 acts as a bridging factor to various F-box proteins that dictate substrate specificity for the entire complex (11). Within the context of the CUL1 scaffold, F-boxes, such as β-TRCP1, SKP2, and FBW7, target IκBα, p27, and cyclin E, respectively, for ubiquitination and subsequent degradation by the proteasome (3).

Database searches reveal eight members of the mammalian cullin family, CUL1, CUL2, CUL3, CUL4A, CUL4B, CUL5, CUL7, and PARC. With the exception of PARC, all of these cullins have previously been shown to form complexes similar to the CUL1-based SCF complex (3). Although all of these complexes contain RBX1 and are modified by NEDD8, the CUL2-, CUL3-, CUL4A-, CUL4B-, and CUL5-based complexes contain analogs of the SKP1 bridging factor and non-F-box substrate specificity factors. The CUL2 and CUL5-based complexes replace SKP1 with elongin B and elongin C, and they target substrates, such as hypoxia-inducible factor 1α and APOBEC3G, for ubiquitination through SOCS box proteins, such as VHL and the human immunodeficiency virus Vif protein (22, 34). CUL4-based complexes utilize DDB1 and DDB2 to bridge to specificity factors such as hDET1, which has been reported to target c-JUN for ubiquitination, and CUL3-based complexes use BTB proteins as both bridging proteins and substrate specificity factors (7, 8, 23, 25, 31, 33).

Although CUL7-based complexes are very similar to CUL1-based complexes based on RBX1, SKP1, and F-box binding, recent reports suggest that these two complexes bind to different accessory proteins and distinct subsets of F-box proteins (1, 6). Glomulin (FAP68) is unique to the CUL7 complex, and although overexpressed FBXW8 (FBW6, FBX29) can bind both CUL7 and CUL1, it binds more strongly to CUL7, with coexpression of SKP1 and FBXW8 increasing FBXW8 binding to CUL7 but not CUL1 (1). In addition, targeted deletion of *Cul7* results in a loss of FBXW8 stability, further supporting the specificity of FBXW8 for CUL7 (1). Finally, CUL7 contains multiple domains outside of the cullin homology domain that suggest that CUL7 can form unique SCF-like complexes (1, 6).

Although the cullin complexes are diverse in structure and substrates, targeted deletions of cullins 1, 3, 4A, and 7 in the mouse have demonstrated each complex's importance in development. Deletion of *Cul1* results in embryonic lethality by embryonic day 5.5, and deletions of *Cul3* or *Cul4a* result in embryonic lethality before embryonic day 7.5 (4, 17, 26, 30). Despite displaying a milder phenotype than the other cullin

* Corresponding author. Mailing address: Dana-Farber Cancer Institute, Mayer Building 457, 44 Binney Street, Boston, MA 02115. Phone: (617) 632-3825. Fax: (617) 632-4760. E-mail: james_decaprio@dfci.harvard.edu.

† Present address: Tokatsu-Tsujinaka Hospital, 946-1 Neda, Abikoshi, Chiba, 270-1168, Japan.

knockouts, *Cul7* knockout mice exhibit neonatal lethality with reduced size and possible vascular defects (1). Presumably the defects in the development of *Cul1*, *Cul3*, *Cul4a*, and *Cul7* knockout mice result from the inability of the deleted cullins to degrade their normal substrates.

The least-characterized mammalian cullin was recently identified as a *PAR*kin-like, *C*ytoplasmic, p53 binding protein (PARC) (20). Although it was suggested that PARC could serve as an E3 ubiquitin ligase, no ubiquitination activity towards p53 was demonstrated. Instead, it was proposed that PARC functioned to sequester p53 in the cytoplasm, preventing p53 from inducing growth arrest and apoptosis (20). PARC is highly homologous to CUL7 throughout its sequence, sharing up to 60% identity in several domains, although PARC differs from CUL7 in the presence of a "spacer domain" of unknown function and a C-terminal RING-IBR-RING domain. Like CUL7, PARC has several discrete domains present in other proteins found in E3 ligase complexes, such as HERC2, APC10/DOC1, and Parkin (1, 6, 9, 16, 29). Further sequence analysis suggests that PARC is the evolutionary precursor of CUL7, since only PARC, and not CUL7, sequences are present in the *Danio rerio* and *Takifugu rubripes* databases.

Here we show that CUL7 and PARC can each form homodimers, as well as forming heterodimers with each other, and that a complex containing PARC can bind p53. Furthermore, through the targeted deletion of *Parc* and the previously published deletion of *Cul7* in the mouse, we demonstrate that the PARC complex is not required for mouse viability, and CUL7 and PARC functions are at least partially nonoverlapping. Additionally, *Parc* deletion has no discernible effect on p53 stability, on the induction of p53 target genes, or on p53 localization.

MATERIALS AND METHODS

Cloning. A partial *PARC* cDNA, KIAA0708, was obtained from the Kazusa DNA Research Institute. The sequence of the missing 5′ region of *PARC* was determined by two cycles of 5′ rapid amplification of cDNA ends, and the resulting sequence information was used to generate a full-length cDNA of *PARC* by PCR from a fetal brain cDNA library. The full-length cDNA was cloned into pcDNA3.0 HA using BamHI and NotI, and mutations introduced by PCR were corrected by replacing sequences with expressed sequence tags, KIAA0708 and IMAGE no. 1351950. An intron present in IMAGE no. 1351950 was removed using a fragment from the full-length *PARC* generated by PCR.

The short hairpin RNA (shRNA) vector pTU6IIa(−) was generated from pBS KS. A U6 promoter containing a TetO element overlapping the TATA box and containing an AgeI site at the initiating site of the U6 RNA was generated by PCR (21). Tet-responsive U6 was cloned into pBS KS using EcoRI and XhoI. A blasticidin resistance cassette driven by the simian virus 40 (SV40) promoter was inserted nondirectionally into the resulting plasmid at the SacII site. pTU6IIa(−) contains this cassette in the opposite orientation from the Tet-U6 promoter. shRNA constructs targeting *PARC* were cloned from annealed oligonucleotides into pTU6IIa(−) using the AgeI and XhoI sites. The shRNA used in this paper corresponds to GGAGTGTCCTGAAGTGTGGGGAAGTGGGCTATGCCC ACTTCCCCACACTTCAGGACACTCC.

Cell culture and γ-irradiation. U-2 OS cells stably expressing an shRNA directed against *PARC* were constructed by cotransfection of pTU6IIa(−) sh281#2 and pcDNA3.0 TetR. Stable clones were selected in 10 μg/ml blasticidin (Invitrogen) and 1 mg/ml G418 (Cellgro). Multiple clones tested positive for PARC depletion, but no clones responded to tetracycline. TetR expression was also undetectable.

Mouse embryo fibroblasts (MEFs) were generated from embryos isolated at embryonic day 14.5. To generate polyclonal MEFs expressing SV40 large T antigen, cells were transduced with the pLB(N)CX-T retroviral vector and selected in 10 μg/ml blasticidin (Invitrogen). For irradiation experiments, fully confluent plates of MEFs were irradiated with 20 Gy from a ^{137}Cs source and harvested at the indicated time points. All transfections were performed using Lipofectamine Plus (Invitrogen). All cells were cultured in Dulbecco's modified Eagle's medium containing 10% Fetalclone serum (HyClone).

Antibodies. The rabbit anti-PARC antibodies BL616, BL617, and BL920, which recognize epitopes within the N-terminal 50 residues, C-terminal 50 residues, and residues between 700 and 750 amino acids, respectively, were from Bethyl Laboratories (Montgomery, TX). Affinity-purified anti-CUL7 (h1557, BL653, and BL1541) antibodies to epitopes mapping between amino acids 1658 to 1676, 1500 to 1550, and 1648 to 1698, respectively, were also produced by Bethyl Laboratories. Additional monoclonal antibodies used for immunoprecipitation and Western blotting include anti-hemagglutinin (HA) (12CA5 and HA-11; Covance), anti-T7 (Novagen), anti-Myc (9B11; Cell Signaling Technology), anti-p53 (Ab-4/Pab122; Neomarkers), anti-MDM2 (2A10; Calbiochem), anti-p21 (HZ52/Ab-5; Neomarkers), and anti-Vinculin (hVin1; Sigma). Rabbit polyclonal anti-Lamin A (Cell Signaling Technology) and anti-PTEN (Cell Signaling Technology) were used for Western blotting. Purified, nonspecific rabbit immunoglobulin G (IgG) (Bethyl) was used as a control for immunoprecipitations. For indirect immunofluorescence microscopy, a mixture of four monoclonal antibodies to p53 (Pab122/Ab-4 [Neomarkers], DO-7/Ab-5 [Neomarkers], Pab240/Ab-1 [Neomarkers], and Pab1620/Ab-5 [Calbiochem]) was used in conjunction with rhodamine-conjugated goat anti-mouse secondary antibody (Molecular Probes).

Immunoprecipitation, Western blotting, and mass spectrometry. U-2 OS cells or MEFs were washed twice in phosphate-buffered saline before lysis in either NET-N (20 mM Tris, pH 8, 100 mM NaCl, 1 mM EDTA, 0.5% NP-40) or EBC (50 mM Tris, pH 8, 120 mM NaCl, 0.5% NP-40) containing a 1× concentration of protease inhibitor cocktail set I (Calbiochem). Extracts were cleared by centrifugation at 12,000 × *g* for 10 min, and protein concentrations were determined by Bradford Assay (Bio-Rad). Nuclear and cytoplasmic extracts were generated using NE-PER (Pierce).

For immunoprecipitation, all antibodies were used with protein A Sepharose beads, and rabbit polyclonal antibodies were used at a concentration of 2 μg per 1 mg of total protein. Immunoprecipitations were performed for 3 h or more at 4°C, and the subsequent immunoprecipitates were washed three times with NET-N or EBC before boiling in sodium dodecyl sulfate (SDS) sample buffer. Whole-cell lysates and immunoprecipitates were separated by SDS-polyacrylamide gel electrophoresis (PAGE) and transferred to nitrocellulose membranes (Bio-Rad) for Western blotting. Membranes were blocked in 5% milk–Tween 20–Tris-buffered saline before Western blotting was performed. Detection of proteins was accomplished using the appropriate secondary antibodies conjugated to horseradish peroxidase (Pierce) at a 1:5,000 dilution in 5% milk–Tween 20–Tris-buffered saline. Western blots were developed using enhanced chemiluminescence (Super Signal; Pierce).

In the experiments leading to the identification of human PARC (hPARC) as a CUL7-interacting protein, A2P2 cells were starved in methionine- and cysteine-free medium for 1 h prior to addition of [^{35}S]methionine at a concentration of 1 mCi per ml (1). Cells were labeled for 3 h before harvesting for immunoprecipitation using HA-11 antibody (Covance). The large-scale preparation used to identify PARC by mass spectrometry is described elsewhere (1). Mass spectrometry yielded the peptide sequence LQQETQPFLLLLR, corresponding to hPARC amino acids 988 to 1000.

Generation of *Parc*$^{-/-}$ mice. A 500-bp probe from coding exon 1 of the PARC genomic sequence was generated from PCR of 129/C57BL/6 mouse genomic DNA using the PCR primers GAACGGCGTGCAGGGAACCTTCTGGTA CCC and CCAGAGCCTGGAGCATCTTGCCTGCACTCC. This probe was used to screen a mouse 129/Sv/En/Tac genomic bacterial artificial chromosome (BAC) library, and four BACs containing PARC genomic DNA were identified (ResGen). PCR from the BAC templates was used to generate a 2.3-kb EcoRI-XhoI fragment containing coding exons 2 and 3, a 1.9-kb SacII-SmaI fragment containing coding exons 4 to 6 with the 3′ *loxP* site, and a 4.5-kb XmaI-SnaBI fragment containing coding exon 7 for cloning into the pGEM-T Easy vector (Promega). The EcoRI, XhoI, SacII, SmaI/XmaI, and 3′ *loxP* sites were introduced by PCR (LA Taq; Takara), and the primer sequences used in the amplification of these fragments are available upon request. The sequence of all coding exons was determined in pGEM-T Easy before the fragments were subcloned into the targeting vector pKOII (2). The fragments containing exons 2 to 3 and exons 4 to 6 were cloned with the restriction sites introduced by PCR as indicated above. The 4.5-kb fragment was cloned using the XmaI site introduced by PCR and a NotI site introduced from pGEM-T Easy. This NotI site was used to linearize the targeting vector prior to electroporation. The sequence of all exons contained in the targeting vector was reconfirmed before electroporation of embryonic stem (ES) cells and selection with G418. The correct integration of the targeting vector was confirmed in one ES cell clone by Southern blotting, PCR, and sequencing across the 3′ *loxP* site of the targeted allele. The PCR primers used in screening were CACAGTCAGCTGCTATGAAGCAGC

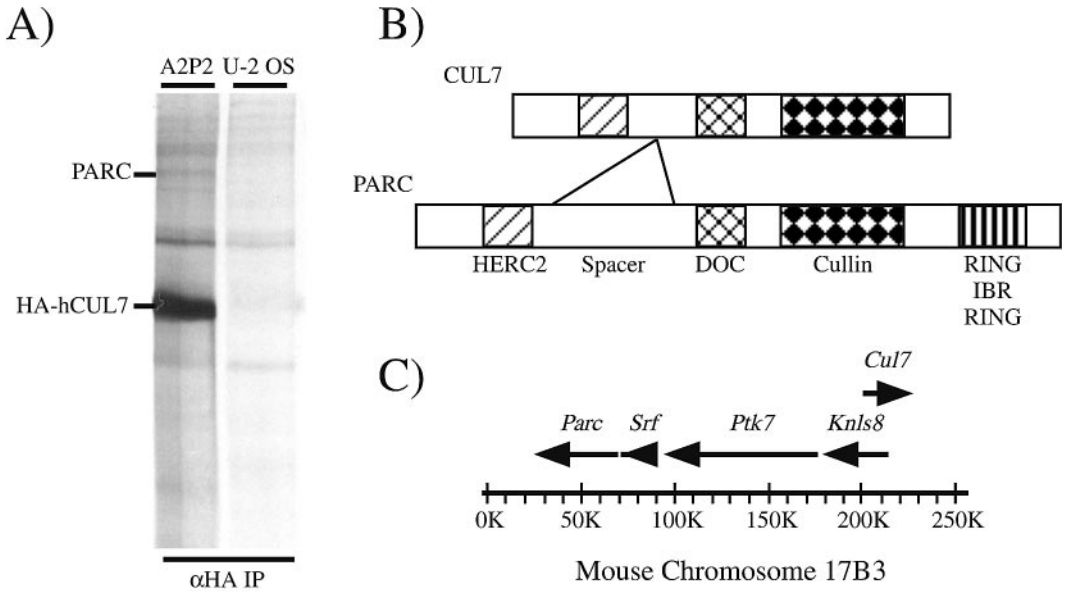

FIG. 1. Identification of PARC as a CUL7-interacting protein. (A) A2P2 cells stably overexpressing HA-hCUL7 were labeled for 3 h with [^{35}S]methionine. Anti-HA (HA-11) immunoprecipitations (IP) from A2P2 or U-2 OS lysates were subjected to SDS-PAGE and autoradiography, revealing a specific interacting protein at 280 kDa, which was later identified as PARC. (B) CUL7 and PARC are highly homologous over their shared regions, with approximately 60% amino acid identity. PARC contains two domains not present in CUL7, including a "spacer" domain with no homology to other known proteins and a C-terminal RING-IBR-RING domain. CUL7 and PARC share homologies to other known proteins, such as HERC2 (40% identity, 65% homology), APC10DOC1 (25% identity, 47% homology), and the cullin (25% identity, 40% homology) family of proteins. (C) In both the mouse and human genomes, *Cul7* and *Parc* are arranged in a head-to-head fashion. They are separated by approximately 130 kb of genomic DNA containing several known genes, including *Knsl8*, *Ptk*, and *Srf*. The *Parc* locus extends from base 44814756 to 4482168, while the *Cul7* locus extends from base 44656630 to 44676889.

CCTGTA and CTGCTAAAGCGCATGCTCCAGACTGCCTTG. To generate chimeras, correctly targeted ES cells were injected into C57BL/6 blastocysts and transferred into pseudopregnant foster mothers. The chimeric mice were backcrossed with C57BL/6 mice to demonstrate germ line transmission or with C57BL/6 mice carrying an *EIIA-Cre* transgene to confirm germ line transmission and generate the null allele (15). *Parc*$^{+/-}$ *EIIA-Cre*$^{+/-}$ mice were backcrossed to C57BL/6 mice to remove the Cre transgene and backcrossed once more to the C57BL/6 background before subsequent mating to generate homozygous null animals. Genotyping for *EIIA-Cre* was performed using the PCR primers ATG TCCAATTTACTGACCGTACACCAAAAT and ACGATGAAGCATGTTTA GCTGGCCCAAATG. Subsequent genotyping for PARC was performed by Southern blotting using the probes above and by PCR using the primers ACT GAAGAACAGGTGGCTGTCAGTTAGACA, GGAGGCAGCTACTGGTG AGTTTGGTTCTGG, and GGTAGCATGGCTTTAAGCCTGGCTCTTAAG. The DNA for genotyping was generated from tails using Purgene kits (Gentra Systems). The deleted allele is officially designated *Parc*^{tm1Jdec}.

Immunofluorescence microscopy and BrdU staining. For immunofluorescence experiments, cells were plated onto coverslips 24 h prior to staining. MG132-treated cells were treated with 25 μM MG132 6 h prior to processing. Cells were fixed in 10% formalin–2% sodium acetate and permeabilized in 0.5% Triton X-100–3% goat serum–PBS for staining with the indicated antibodies. For anti-BrdU staining, cells were irradiated with 7.5 Gy and labeled with BrdU for 1.5 h at 14 h postirradiation. After BrdU labeling, cells were fixed in 70% ethanol prior to denaturation of DNA in 2N HCl. Blocking was performed with 3% bovine serum albumin in 0.1 M $Na_2B_4O_7$, pH 8.5, before incubation with the anti-BrdU-fluorescein isothiocyanate (FITC) conjugate or an isotype control-FITC conjugate (BD Pharmingen). Subsequently, cells were stained with propidium iodide and analyzed by fluorescence-activated cell sorting (FACS).

RESULTS

Isolation of CUL7-associated proteins. The previously isolated CUL7 complex contained proteins consistent with those in other SCF-like complexes, including SKP1, RBX1, and FBXW8 (1, 6). However, the presence of glomulin in this complex and the existence of multiple conserved domains outside of the cullin homology domain of CUL7 suggested that additional proteins might be part of the complete CUL7 complex (Fig. 1B) (1). To identify CUL7 binding proteins, U-2 OS cells stably expressing HA-tagged human CUL7 (HA-hCUL7) (A2P2 cells) were metabolically labeled with [^{35}S]methionine, treated with increasing amounts of the proteasome inhibitor MG132, and immunoprecipitated with anti-HA antibody (1). In addition to a 58-kDa band that contains FBXW8 and glomulin, the HA immunoprecipitation for HA-hCUL7 specifically coimmunoprecipitated a protein of approximately 280 kDa (Fig. 1A). A previously described preparative scale immunoprecipitation from A2P2 lysates generated sufficient amounts of the 280-kDa protein to allow identification by mass spectrometry, which yielded one peptide (LQQETQP FLLLLR) corresponding to KIAA0708, later named hPARC (1).

Specific binding of CUL7 to PARC. Initial database searches using the PARC sequence revealed an extremely high homology to CUL7. PARC and CUL7 are homologous over their entire length, sharing approximately 60% identity and 70% homology over their shared domains (Fig. 1B). Notably, PARC differs from CUL7 in the presence of a "spacer" domain of unknown function and a C-terminal RING-IBR-RING. In addition to exhibiting homology to each other, PARC and CUL7 share regions of homology with other proteins in the database, including HERC2, APC10DOC1, and the cullins (Fig. 1B) (1, 6, 9, 16). Notably, all of these proteins are linked with E3 ubiquitin ligase function, suggesting that PARC and CUL7 may both function as E3 ubiquitin ligases. Although multiple proteins have been noted to contain combinations of these

domains in tandem, HERC2, PARC, and CUL7 are unique in the presence of three or more such domains (9).

Subsequent searches of the genomes of lower organisms indicated that PARC is most likely the evolutionary precursor of CUL7. *PARC* first appears in the genomes of *D. rerio*, *Xenopus tropicalis*, and *T. rubripes*, while *CUL7* appears only in mammalian genomes, suggesting that *PARC* is the evolutionary precursor for *CUL7*. BLAST searches of the *D. rerio* expressed-sequence-tag and genomic databases with human PARC revealed extensive conservation throughout the entire PARC primary sequence. These *D. rerio* sequences can clearly be distinguished from that of CUL7 due to characteristic insertions in the PARC N terminus (i.e., residues 96 to 102) that are not present in CUL7 and additional PARC-specific sequences, such as those of the "spacer" and RING-IBR-RING domains, that are not found in CUL7. The two genes are arranged in a head-to-head fashion on human chromosome 6 and mouse chromosome 17, and they are separated by approximately 130 kb of genomic DNA, containing several confirmed genes, including *Srf*, *Ptk*, and *Knsl8* (Fig. 1C).

The apparent dimerization of hCUL7 with its close homolog hPARC suggested that hCUL7 could also form homodimers. To confirm the heterodimerization of hCUL7 and hPARC and to look for homodimerization of hCUL7, HA-tagged hCUL7 and HA-tagged hPARC were cotransfected with T7-tagged hCUL7 for analysis by coimmunoprecipitation and Western blotting using anti-T7 and anti-HA antibodies. Immunoprecipitations for T7-hCUL7 coprecipitated both HA-hCUL7 and HA-hPARC, while the reciprocal immunoprecipitations for HA-hCUL7 and HA-hPARC precipitated T7-hCUL7, confirming the formation of CUL7-PARC heterodimers and CUL7-CUL7 dimers (Fig. 2A). The homodimerization of hCUL7 and the extensive homology between CUL7 and PARC suggested that PARC could also form homodimers. To test for hPARC homodimerization, cells were transfected with HA-tagged hPARC and Myc-tagged hPARC for analysis by coimmunoprecipitation and Western blotting. Reciprocal immunoprecipitations for Myc-hPARC or HA-hPARC coprecipitated HA-hPARC and Myc-hPARC, respectively, confirming homodimerization of PARC (Fig. 2B).

To confirm that the interaction between CUL7 and PARC was not the result of the transient overexpression of either protein, polyclonal, monospecific antibodies were generated against hCUL7 and hPARC to test the interaction of endogenous protein by coimmunoprecipitation and Western blotting. Immunoprecipitation of endogenous CUL7 from U-2 OS cells revealed coprecipitation of PARC, and immunoprecipitation of PARC using antibodies generated to two distinct epitopes resulted in the coprecipitation of CUL7, confirming the dimerization of endogenous CUL7 and PARC (Fig. 2C). The specificity of the anti-CUL7 and anti-PARC antibodies was demonstrated by the inability of purified rabbit IgG to immunoprecipitate either protein. Additionally, a U-2 OS cell line stably expressing an shRNA directed against *PARC* demonstrates the specificity of the anti-PARC BL617 antibody for Western blotting. The presence of an endogenous CUL7-PARC complex was also confirmed in MEFs by immunoprecipitation with antibodies specific for each protein followed by Western blotting (Fig. 2D). In MEF whole-cell lysates and immunoprecipitations, a nonspecific, high-molecular-weight band appears above PARC upon Western blotting. This band was unaffected by *Parc* knockout (see below), and it was immunoprecipitated nonspecifically by rabbit IgG (Fig. 2D) or any other antibody tested (see below). Notably, human PARC and mouse PARC show no size difference in gel migration by SDS-PAGE, so lysates from the U-2 OS and U-2 OS short hairpin PARC (shPARC) cells were included in subsequent experiments as a reference standard for mouse PARC (see below).

Generation of *Parc*$^{-/-}$ mice. To understand the function of the CUL7-PARC complex and the potential PARC-PARC complex, we generated a targeted deletion of *Parc* in the mouse model. Previously we reported that mice with a targeted deletion of *Cul7* are inviable, exhibiting neonatal lethality with reduced size and vascular defects (1). Because all previous cullin knockouts resulted in embryonic or neonatal lethality, the *Parc* gene-targeting vector was designed to conditionally delete coding exons 4 to 6 when the Cre recombinase is expressed, causing exon 3 to splice into exon 7 where the message is out of frame with multiple stops (Fig. 3A).

Mouse ES cells were electroporated with the linearized construct and selected for G418 resistance. Correct integration of the targeting construct was confirmed by Southern blotting using a probe located 5′ to the short arm of the targeting construct and a PCR screen (data not shown). The probe used for ES cell screening was subsequently used for all genotyping Southern blots. Correct integration of the 5′ end of the targeting construct was confirmed in two ES cell clones, and the presence of the 3′ *loxP* site was confirmed in one clone by sequencing. Chimeric mice generated from injection of this ES cell clone into a C57BL/6 blastocyst were mated to C57BL/6 mice to demonstrate germ line transmission or to C57BL/6 mice carrying an *EIIA-Cre* transgene to demonstrate germ line transmission while generating the null allele (Fig. 3B) (15). *Parc*$^{+/-}$ *EIIA-Cre* mice were backcrossed to C57BL/6 to remove the *EIIA-Cre*, and these *Parc*$^{+/-}$ mice were backcrossed again to the C57BL/6 background before breeding heterozygous mice to generate *Parc*$^{-/-}$ mice.

Mating of *Parc*$^{+/-}$ mice generated *Parc*$^{-/-}$ mice, as shown by Southern blotting and PCR of tail DNA from 3-week-old mice (Fig. 3C and D). The number of *Parc*$^{-/-}$ mice obtained was not significantly different from the expected Mendelian ratio (15 *Parc*$^{-/-}$ mice, 20 *Parc*$^{+/-}$ mice, and 12 *Parc*$^{+/+}$ mice; $\chi^2 = 1.246$; $P = 0.4903$). *Parc*$^{-/-}$ mice exhibit no physical deformities or growth defects, and they appeared phenotypically normal when compared to wild type or heterozygous littermates. No health problems have emerged as these mice have aged to more than 400 days. Additionally, both male and female *Parc*$^{-/-}$ mice are fertile, since crosses involving knockouts yielded consistently normal litter sizes.

To confirm that *Parc*$^{-/-}$ mice were indeed null for PARC, MEFs were generated from 14.5-day embryos from *Parc*$^{+/-}$ × *Parc*$^{+/-}$ crosses. The genotypes of the MEFs were confirmed by Southern blotting and PCR (Fig. 4A; also data not shown). *Parc*$^{+/-}$ and *Parc*$^{-/-}$ MEFs displayed no apparent growth defects in culture when compared to MEFs from wild-type littermates. Matched littermate MEFs were used for subsequent Western blotting for the PARC protein. Western blots of lysates prepared from *Parc*$^{+/+}$, *Parc*$^{+/-}$, and *Parc*$^{-/-}$ MEFs demonstrated that a null allele of *Parc* was generated, and

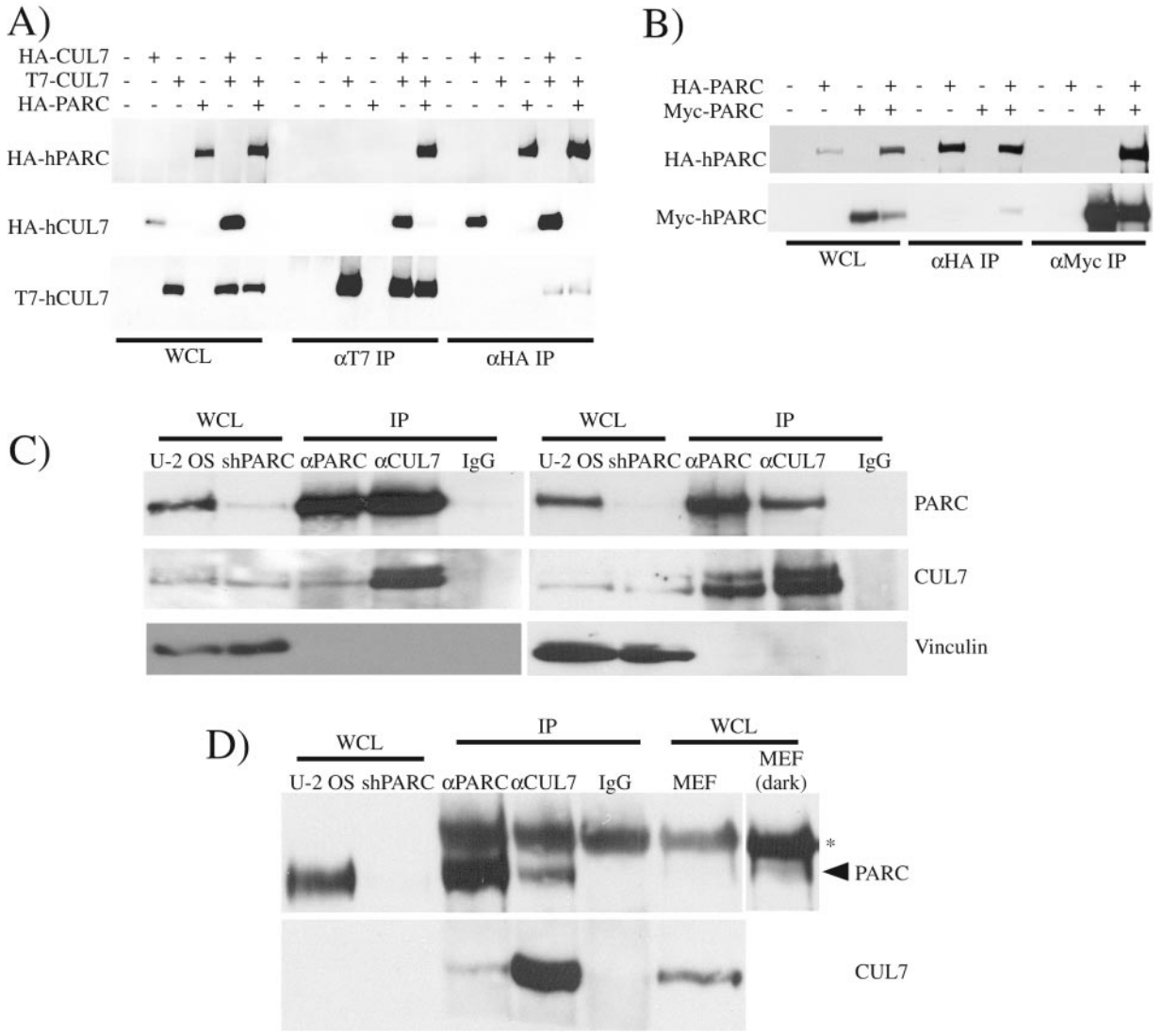

FIG. 2. CUL7 and PARC form heterodimers and homodimers. (A) U-2 OS cells were transiently transfected with T7-hCUL7, HA-hCUL7, and HA-hPARC. Lysates were immunoprecipitated (IP) and then Western blotted with anti-HA (12CA5) (αHA) and anti-T7 (αT7) antibodies as indicated. Whole-cell lysates (WCL) demonstrate expression of the transfected proteins. (B) U-2 OS cells were transfected with HA-hPARC and Myc-hPARC. Lysates were immunoprecipitated and then Western blotted with anti-HA (12CA5 IP, HA-11 western) (αHA) and anti-Myc (9B11) (αMyc) antibodies. (C) U-2 OS cell lysates were immunoprecipitated with anti-CUL7 (h1557), nonspecific rabbit IgG, and either anti-PARC (BL920) (left panel) or anti-PARC(BL617) (right panel). Immunoprecipitates were analyzed by Western blotting with anti-CUL7(BL653) (αCUL7), anti-PARC(BL617) (αPARC), and antivinculin. One hundred twenty micrograms of whole-cell extract from U-2 OS and U-2 OS shPARC cells was included as a control for anti-PARC Western blotting. (D) MEF lysates were immunoprecipitated with anti-CUL7 (h1557) (αCUL7), anti-PARC(BL617) (αPARC), and nonspecific rabbit IgG. Immunoprecipitates were analyzed by Western blotting with anti-CUL7 (BL1541) and anti-PARC(BL617). The MEF WCL lane (first and second from right) contains 150 μg of total protein, and a darker exposure is provided on the right. Seventy micrograms of whole-cell extract from U-2 OS and U-2 OS shPARC cells was included as a size standard for distinguishing between mouse PARC and a nonspecific background band (asterisk).

Parc$^{-/-}$ tissues do not contain PARC protein (Fig. 4B). The absence of PARC protein from *Parc*$^{-/-}$ MEFs was further confirmed by the absence of PARC from anti-PARC immunoprecipitates using antibodies against three distinct epitopes in the N terminus, C terminus, and an internal region, as well as the failure of anti-CUL7 antibody to coimmunoprecipitate PARC (Fig. 4C). The previously noted, nonspecific, high-molecular-weight band migrating slower than PARC in mouse cells was present in *Parc*$^{-/-}$ MEFs, and it could be distinguished from PARC by the inclusion of lysates from U-2 OS and U-2 OS shPARC cells as a size standard. Western blotting of whole-cell extracts and anti-PARC immunoprecipitations also revealed that heterozygous MEFs contained a reduced level of PARC relative to wild-type MEFs. Western blotting for CUL7 from lysates of *Parc*$^{-/-}$ MEFs showed a slight decrease in the expression of CUL7 (Fig. 4B).

PARC-CUL7-p53 complex. PARC was reported to bind p53 in a cytoplasmic complex in human cells (20). To confirm binding of PARC to p53 in mouse cells, we performed immunoprecipitations for PARC from wild-type, *Parc*$^{-/-}$, and

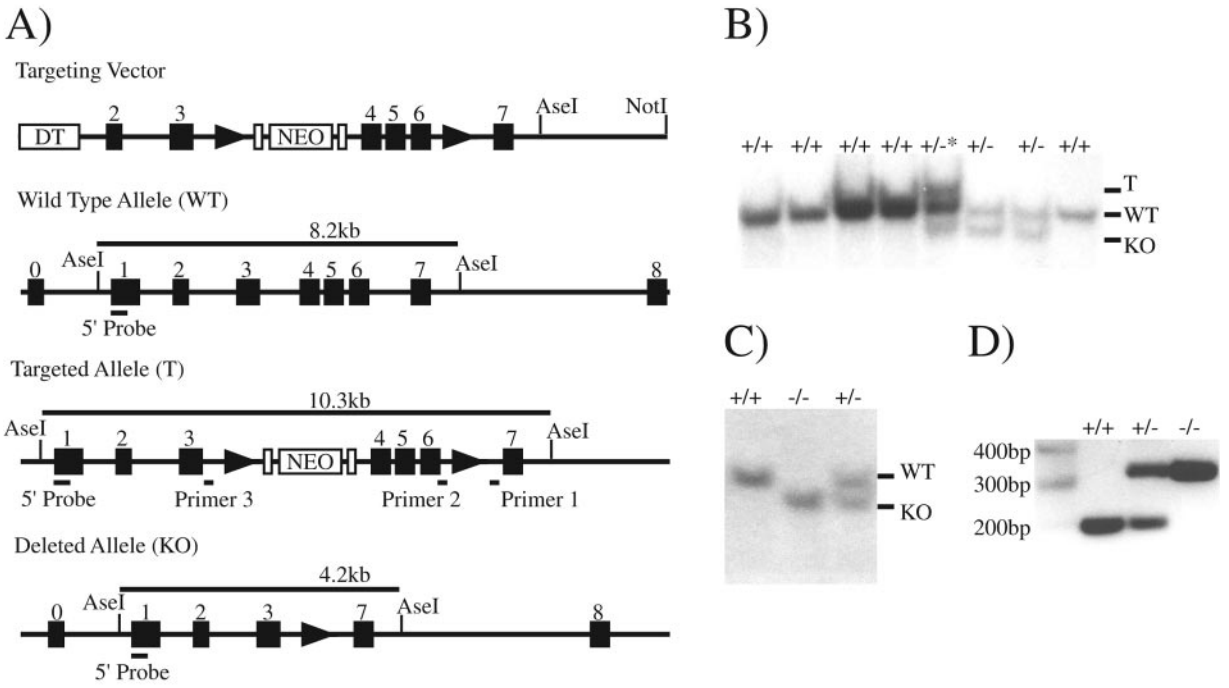

FIG. 3. Targeted disruption of *Parc*. (A) A partial map of the targeting vector, the 5′ end of the genomic *Parc* locus (WT), the targeted allele (T), and the deleted allele (KO). Exon 0 is a noncoding exon, and exon 1 contains the translation start site. Using a probe from exon 1, Southern blotting of an AseI digest was used to screen ES cells and genotype mice. Primers used to genotype mice are indicated. Filled triangles and open rectangles indicate *loxP* and *Frt* sites, respectively. DT is diphtheria toxin, and NEO is neomycin acetyltransferase. (B) Southern blot of an AseI digest of tail DNA from the progeny of a chimeric male and a C57BL/6 *EIIA-Cre* female. The asterisk indicates incomplete excision of the targeted allele. (C) Southern blot of an AseI digest of tail DNA from the progeny of a cross of two $Parc^{+/-}$ mice. (D) Genotyping PCR from the tail DNA of the progeny of a cross of two $Parc^{+/-}$ mice. The wild-type allele was detected by the 200-bp PCR fragment from primers 1 and 2, and the deleted allele was detected by the 360-bp PCR fragment from primers 1 and 3.

$Trp53^{-/-}$ MEFs. Human CUL7 also binds p53 (Kasper et al., unpublished data), so PARC immunoprecipitations were also performed from $Cul7^{-/-}$ MEF lysates to determine if PARC binding to p53 was dependent on CUL7. Western blotting of PARC immunoprecipitates from wild-type and $Cul7^{-/-}$ MEFs revealed that PARC bound p53, and this binding was independent of CUL7 (Fig. 5A). Notably, $Trp53^{-/-}$ and $Cul7^{-/-}$ MEFs expressed lower levels of PARC than wild-type MEFs (Fig. 4B and Fig. 5A). The level of PARC expression in these MEFs was less than the levels found in $Parc^{+/-}$ MEFs (Fig. 4B).

The observation that p53 binds to PARC raised the possibility that p53 could serve as a substrate for the potential E3 ligase activity of PARC. To address this possibility, the effect of *Parc* deletion on p53 stability was examined. First, the steady-state levels of p53 in primary $Parc^{+/+}$, $Parc^{+/-}$, and $Parc^{-/-}$ MEFs were analyzed by Western blotting. In early-passage +/+, +/−, and −/− MEFs, p53 was nearly undetectable due to its short half-life (Fig. 5B). Treatment of these MEFs with the proteasome inhibitor MG132 led to increased levels of p53. Similarly, expression of SV40 large T antigen in these MEFs led to the stabilization and increased expression of p53 in MEFs of all genotypes. In mock-treated, MG132-treated, and T-antigen-expressing MEFs, *PARC* deletion appeared to have no detectable effect on the steady-state levels of p53 (Fig. 5B). In addition, $Parc^{-/-}$ MEFs did not show any changes in the steady-state expression levels of p53 downstream targets, such as MDM2 and p21, compared to +/+ or +/− MEFs.

While no differences were found in the steady-state levels of p53, PARC might control the levels of p53 upon exposure to genotoxic stresses. To test the p53 response to γ-irradiation, wild-type or $Parc^{-/-}$ MEFs were irradiated with 20 Gy and harvested at the indicated time points (Fig. 5C). Wild-type MEFs displayed a characteristic increase in p53 levels beginning at around 45 min after γ-irradiation, followed by a decrease at 180 min. The p53 response in $Parc^{-/-}$ MEFs was indistinguishable from that observed in wild-type MEFs (Fig. 5C). The p53 response of wild-type and $Parc^{-/-}$ MEFs was further confirmed using an antibody to the radiation-induced serine 15 phosphorylation of p53. Additionally, p53 was able to induce increased MDM2 expression by 90 min in both wild-type and $Parc^{-/-}$ MEFs, suggesting that the transactivation function of p53 was normal in $Parc^{-/-}$ MEFs.

Although p53 function appeared intact by the induction of MDM2, we wished to further confirm that the overall biological function of p53 was unaffected by *Parc* deletion. In response to γ-irradiation, MEFs arrest in G_1 phase in a p53-dependent manner. To test the ability of p53 to induce this G_1 arrest in *Parc*-deficient cells, early-passage wild-type, $Parc^{-/-}$ and $Trp53^{-/-}$ MEFs were irradiated and labeled with BrdU 14 h postirradiation before analysis by FACS (Fig. 6). As measured by anti-BrdU and propidium iodide staining, wild-type MEFs showed a decrease in S-phase cells (−10.9%) in response to irradiation, while $Trp53^{-/-}$ MEFs showed no decrease (−0.9%) in S-phase cells in response to irradiation. Despite being early-passage MEFs, the *Trp53*-deficient MEFs

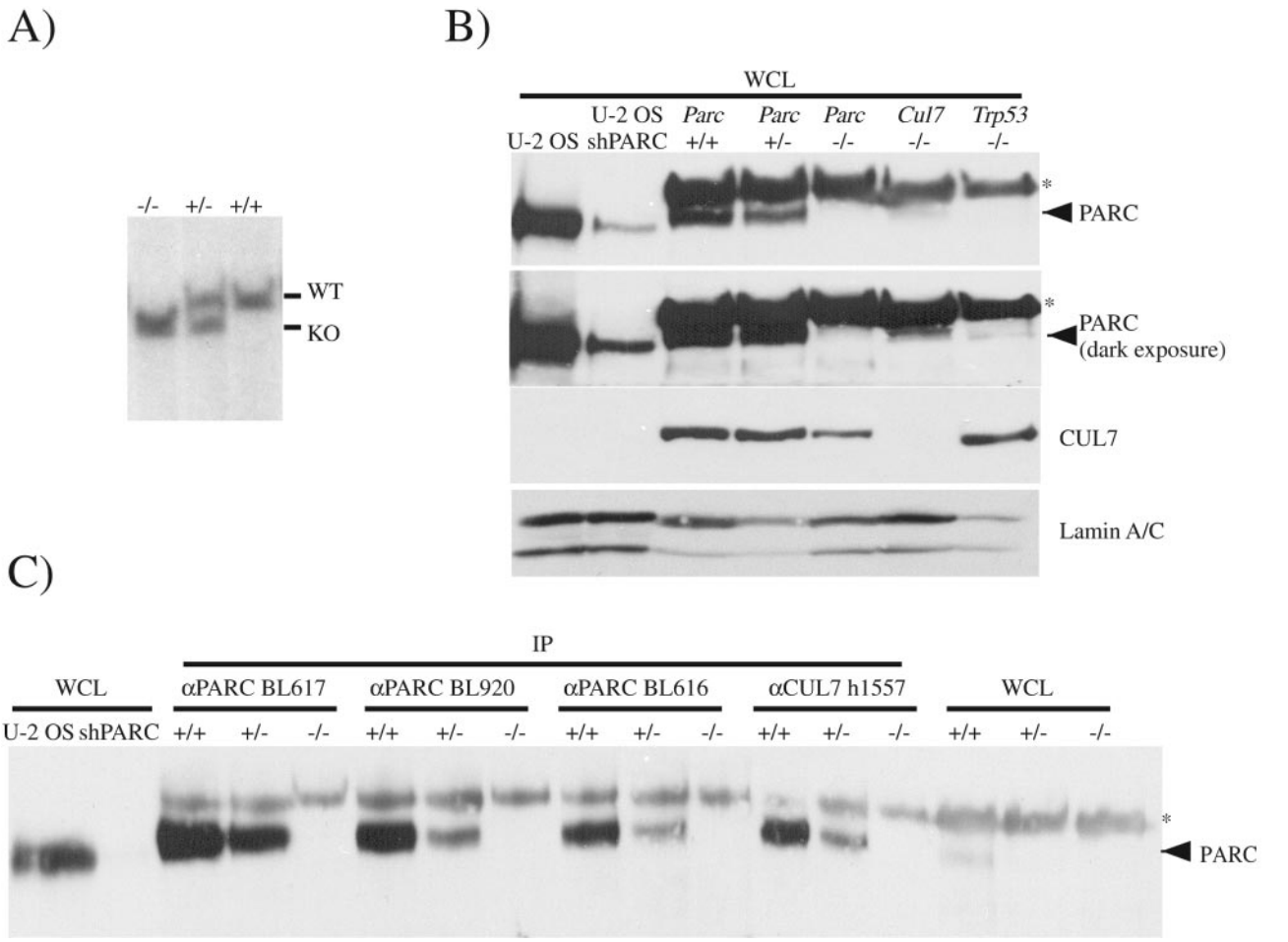

FIG. 4. PARC is not produced in *Parc*$^{-/-}$ tissues. (A) Southern blot of an AseI digest of MEFs derived from embryos of a cross of two *Parc*$^{+/-}$ mice. (B) Western blotting for PARC (BL617), CUL7 (BL1541), and nuclear Lamins A/C was performed on 150 μg of whole-cell lysate from *Parc*$^{+/+}$, *Parc*$^{+/-}$, *Parc*$^{-/-}$, *Cul7*$^{-/-}$, and *Trp53*$^{-/-}$ MEFs. Seventy micrograms of whole-cell lysate of U-2 OS and U-2 OS shPARC cells was included as a size standard for identifying mouse PARC. (C) Lysates from *Parc*$^{+/+}$, *Parc*$^{+/-}$, and *Parc*$^{-/-}$ MEFs were immunoprecipitated with three anti-PARC (αPARC) antibodies (BL616, BL920, and BL617) and anti-CUL7 (αCUL7) (h1557) antibody. One hundred fifty micrograms of whole-cell lysate from each MEF genotype and 70 μg of whole-cell lysate of U-2 OS and U-2 OS shPARC cells are included as expression controls and standards for identifying mouse PARC, respectively. WT, wild type; KO, knockout.

showed a significant increase in 4N and 8N cells. Similarly to wild-type MEFs, *Parc*$^{-/-}$ MEFs displayed an 11.8% decrease in S phase in response to irradiation, indicating normal p53 function in these cells.

Previously it was suggested that PARC functions as a cytoplasmic anchor for p53 and that depletion of PARC resulted in nuclear accumulation of p53 and induction of apoptosis (20). The ability to generate viable *Parc*$^{-/-}$ mice suggested that PARC was not essential to inhibition of p53's apoptotic functions. To examine the effect of *Parc* deletion on the cellular localization of p53, nuclear and cytoplasmic extracts were generated from wild-type and *Parc*$^{-/-}$ MEFs (Fig. 7A). In wild-type and *Parc*$^{-/-}$ MEFs, p53 was found in barely detectable amounts in the nuclear compartment. MG132 treatment of cells prior to extraction increased the amount of nuclear p53 and allowed the detection of a small amount of cytoplasmic p53 in both wild-type and *Parc*$^{-/-}$ MEFs. Notably, no detectable redistribution of p53 from the cytoplasm to the nucleus was observed in either wild-type or *Parc*$^{-/-}$ MEFs. Western blotting for PTEN and nuclear Lamins A and C confirmed proper separation of the cytoplasm from the nucleus and equal loading of protein.

To further examine the effect of *Parc* deletion on p53 localization, immunofluorescence microscopy for p53 was performed on wild-type, *Parc*$^{-/-}$, and *Trp53*$^{-/-}$ MEFs (Fig. 7B). As in Western blots, endogenous, noninduced p53 was undetectable by immunofluorescence in MEFs of all genotypes. MG132 treatment prior to immunostaining allowed the specific detection of p53 in wild-type and *Parc*$^{-/-}$ MEFs but not the in *Trp53*$^{-/-}$ MEF control. In both wild-type and *Parc*$^{-/-}$ MEFs, p53 was detectable only in the nuclear compartment, and no redistribution of p53 from the cytoplasm to the nucleus was apparent.

DISCUSSION

The CUL7-PARC complex. Mammals encode at least eight cullins that all form structurally similar yet unique complexes, sharing some common elements. During an investigation of the

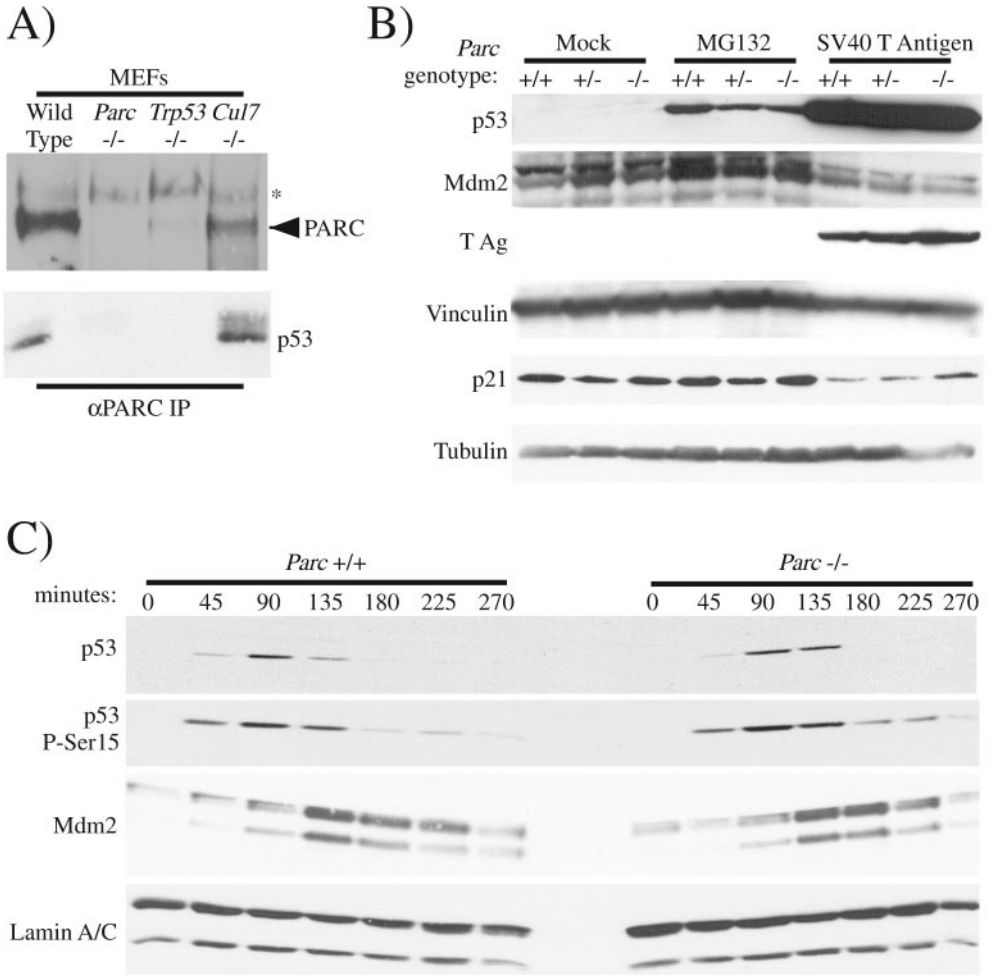

FIG. 5. *Parc* deletion does not affect p53. (A) PARC binds p53 in MEFs. Lysates from $Parc^{+/+}$, $Parc^{-/-}$, $Trp53^{-/-}$, and $Cul7^{-/-}$ MEFs were immunoprecipitated for PARC (BL617) and analyzed by Western blotting for PARC (BL617) and p53 (Pab122) αPARC, anti-PARC. (B) One hundred fifty micrograms of lysates from MEFs, MG132-treated MEFs, and MEFs stably expressing SV40 large T antigen (T Ag) were subjected to Western blotting for p53, MDM2, T Ag, p21, vinculin, and tubulin. p53, MDM2, T Ag, and vinculin blots were performed from the same gel, while p21 and tubulin blots were performed with a second gel. MEF genotypes are as indicated. MG132-treated MEFs were treated with 25 μM MG132 for 6 h before harvesting. (C) *Parc* deletion does not effect the induction of p53 by γ irradiation. $Parc^{+/+}$ and $Parc^{-/-}$ MEFs were irradiated with 20 Gy and harvested at the indicated times. One hundred micrograms of whole-cell extract was loaded per lane, and Western blotting was performed for p53, phosphoserine 15 p53, MDM2, and Lamin A/C.

CUL7 complex, PARC was found to form an endogenous complex with CUL7. Additionally, homodimers of hCUL7 and hPARC were observed in overexpression systems. The ability to form homodimers as well as heterodimers suggests that three distinct complexes containing CUL7 and/or PARC may exist in cells: CUL7-CUL7, CUL7-PARC, and PARC-PARC. This possibility is supported not only by the ability of overexpressed protein to form homodimers and heterodimers but also by data from coimmunoprecipitations of endogenous protein that show not all of PARC is in complex with CUL7 nor is all of CUL7 in complex with PARC.

The viability of $Parc^{-/-}$ mice contrasts with the neonatal lethality of $Cul7^{-/-}$ mice and suggests that the interaction between CUL7 and PARC is not essential for normal development of mice. This observation suggests that although a CUL7-PARC complex forms, only a complex containing CUL7—potentially as a homodimer—is required for development. It is interesting that although CUL7 and PARC are ubiquitously expressed, their expression levels have been reported to vary greatly in certain tissues, which could make the CUL7-to-PARC expression ratio the determining factor in the formation of functional complexes (13, 20). Indeed, the relative expression levels of CUL7 and PARC were substantially different when several different human cancer cell lines were compared (data not shown).

CUL7 binding to PARC represents the first example of cullin dimerization. Several models could explain the functional significance of this interaction. First, CUL7 could be a substrate for PARC-mediated ubiquitination and degradation, or PARC could be a substrate for CUL7-mediated ubiquitination and degradation. However, this possibility seems unlikely given the relative expression levels of each protein in the other's knockout. $Parc^{-/-}$ MEFs express normal or slightly reduced levels of CUL7, and $Cul7^{-/-}$ MEFs show decreased rather than increased levels of PARC. Other explanations for the CUL7-PARC interaction include the requirement of an

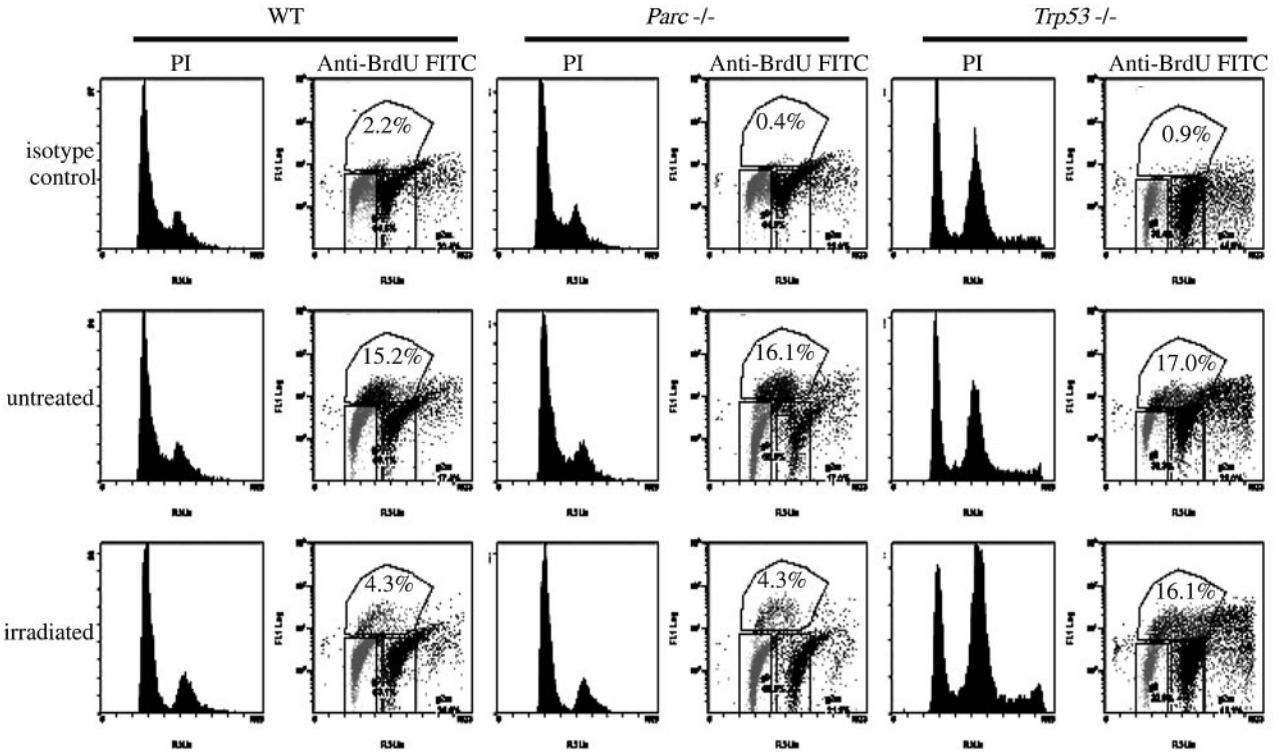

FIG. 6. *Parc* deletion does not affect the ability of p53 to induce G_1 arrest. Wild-type, $Parc^{-/-}$, and $Trp53^{-/-}$ MEFs were irradiated with 7.5 Gy, labeled with BrdU 14 h postirradiation, and analyzed by FACS for anti-BrdU-FITC and propidium iodide. The percentage of cells in S phase for each sample is indicated.

external RING protein (other than RBX1) for certain cullin functions. An SCF complex containing CUL1 and FBXW7 has been reported to bind Parkin (PARK2), a PARC-related RING-IBR-RING protein, to target cyclin E for degradation in neurons, suggesting that other cullins may have RING-IBR-RING binding partners required for subsets of substrates (27). Finally, previous studies have demonstrated hetero- and homodimerization of F-box proteins. In particular, a complex containing human β-TRCP-1 and β-TRCP-2 has been shown to target IκBα for ubiquitination, and a complex containing *Schizosaccharomyces pombe* Pop1 and Pop2 has been shown to target Cdc18 and Rum1 for ubiquitination (14, 28, 32). These

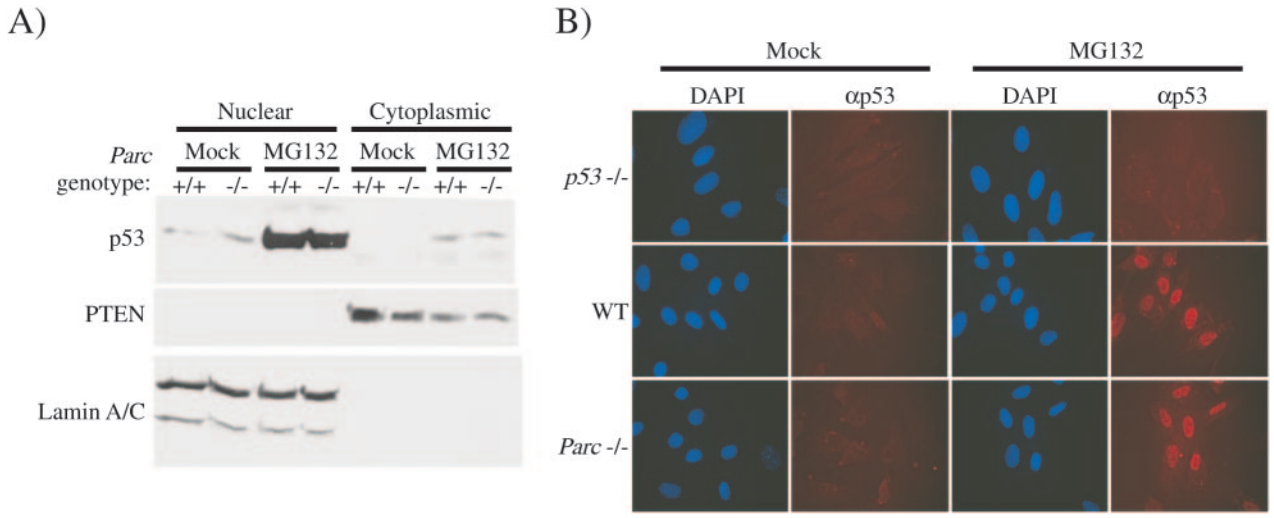

FIG. 7. Deletion of *Parc* does not affect p53 localization. (A) MG132-treated or mock-treated MEFs were subjected to nuclear and cytoplasmic extraction. Two hundred micrograms of cytoplasmic extract and the corresponding percentage of nuclear extract were separated by SDS-PAGE and subjected to Western blotting for p53, PTEN, and Lamin A/C. MG132 treatment was performed at 25 μM for 6 h before harvesting. MEF genotypes are as indicated. (B) Immunofluorescence microscopy using a mixture of monoclonal antibodies (Pab122, Pab240, DO-7, and Pab1620) was performed for p53 in MG132-treated or mock-treated MEFs of the indicated genotypes.

results suggest that the dimerization of CUL7 and PARC could be mediated through F-box proteins and that other cullins, such as CUL1, could form dimers. Notably, dimerization of F-box proteins has been reported only for F-box proteins containing WD-40 repeats, such as β-TRCP1, β-TRCP2, Pop1, and Pop2. The only known F-box for CUL7, FBXW8, is also a WD-40 domain-containing F-box, suggesting that FBXW8 dimerization could mediate the interaction between PARC and CUL7. Attempts to analyze the contribution of F boxes to CUL7 and PARC dimerization will require the identification of all F-boxes that bind CUL7 and PARC.

Parc$^{-/-}$ mice are phenotypically normal. To date, all of the targeted deletions of cullins in mice have resulted in early embryonic lethality, with only the *Cul7* knockout producing lethality at later stages in development (1, 4, 26, 30). In light of the previously observed cullin phenotypes, the high degree of conservation of the *Parc* gene from fish to human, and the inviability of the *Cul7* knockout, the targeted deletion of *Parc* was expected to result in embryonic lethality. However, *Parc*$^{-/-}$ mice were born at a normal Mendelian ratio and exhibit no apparent growth or developmental differences when compared to littermate wild-type animals. Currently it is unclear why *Parc*$^{-/-}$ mice survive when mice lacking *Cul7*, an apparent evolutionary descendant of *Parc*, survive. The fish genome does not appear to contain *Cul7*, and it is likely that fish PARC fulfills a role handled jointly by mouse CUL7 and PARC. Although it is possible that CUL7 could compensate for the loss of PARC in *Parc*$^{-/-}$ mice, it is notable that CUL7 and PARC, though both ubiquitously expressed, are often not highly expressed in the same tissues, suggesting that complementation would require large upregulations of CUL7 that are not observed in knockout MEFs. Unfortunately, it is not possible to generate a *Parc*$^{-/-}$ *Cul7*$^{+/-}$ or a *Parc*$^{-/-}$ *Cul7*$^{-/-}$ embryo or mouse via mating of existing knockout mice, since the two genes are less than 130 kb apart on mouse chromosome 17 (Fig. 1). In order to study the ability of CUL7 to mask *Parc*$^{-/-}$ phenotypes, *Parc*$^{+/-}$ ES cells will require retargeting of *Cul7*.

PARC-p53-CUL7. The survival of Parc$^{-/-}$ mice is surprising not only given the lethal phenotypes of the other cullins and the evolutionary conservation of PARC but also because of previously published reports that depletion of PARC by small interfering RNA leads to apoptosis through p53 relocalization (20). If PARC functioned as an inhibitor of p53 activity, the *Parc* knockout mouse should exhibit a phenotype similar to that of the *Mdm2* knockout, which exhibits early embryonic lethality due to the inability to deactivate p53 (12, 19). However, the survival of the *Parc* knockout mouse and the ability to establish U-2 OS lines stably expressing shRNAs against *PARC* suggest that the reported induction of apoptosis upon depletion of PARC was a nonspecific effect of the single small interfering RNA used (24).

Although a PARC-p53 complex was detectable in MEFs, *Parc* deletion failed to affect p53 stability, target gene induction, or localization. If PARC functioned as an E3 ubiquitin ligase for p53, it would be expected that *Parc*$^{-/-}$ MEFs would exhibit increased steady-state levels of p53, but, unexpectedly, the inverse was true. *PARC*$^{-/-}$ MEFs contained normal levels of p53, while *Trp53*$^{-/-}$ MEFs displayed markedly lower levels of PARC than wild-type MEFs. The ability to upregulate and later downregulate p53 in *Parc*$^{-/-}$ MEFs in response to γ-irradiation also appears intact, suggesting that even when MDM2-ubiquitinated p53 was shuttled from the nucleus to the cytoplasm, PARC has little or no role in p53 degradation following a response to ionizing radiation. Additionally, the observed induction of MDM2 demonstrates that *Parc* deletion has no effect on the transactivation activities of p53 in response to γ-irradiation. Previous reports suggested that PARC negatively regulated p53 by sequestration in the cytoplasm, and the loss of p53 sequestration by PARC caused increased expression of p53 target genes. However, *Parc* deletion had no effect on the levels of p21 and MDM2, and in *Parc*$^{-/-}$ MEFs no change in the ratio of nuclear to cytoplasmic p53 was observed compared to wild-type MEFs, even when the levels of p53 were increased by the addition of MG132. Finally, deletion of *Parc* did not affect the ability of p53 to induce a G_1 arrest following γ irradiation, suggesting that p53 is fully functional in *Parc*$^{-/-}$ MEFs.

The absence of an effect of *Parc* deletion on p53 stability and localization demonstrates that PARC is not necessary for these functions. Although the high degree of homology between PARC and CUL7 and the presence of a CUL7-p53 complex in human cells suggest that CUL7 may be sufficient to properly regulate p53 levels and activity in the absence of PARC, p53 protein levels and activity appear normal in *Cul7*$^{-/-}$ MEFs (data not shown). Notably, these *Cul7*$^{-/-}$ MEFs exhibit normal p53 levels and function even though they express very low levels of PARC.

Several alternative models to the negative regulation of p53 by PARC through sequestration and ubiquitination also exist. Transcription factors such as VP16 require ubiquitination for activity, making it possible that PARC could ubiquitinate p53, thereby increasing transcriptional activity (35). However, the ability of p53 to induce MDM2 in *Parc*$^{-/-}$ MEFs suggests that such an activity is not required for *Mdm2* induction. Additional models also address the apparent discrepancy of the binding of PARC, a cytoplasmic protein, to p53, a predominantly nuclear protein. Cytoplasmic p53 has been reported to translocate to the mitochondria following DNA damage to induce apoptosis (18). It is possible that p53 translocation to the mitochondria could be controlled by PARC binding and modification, since small ubiquitin-like protein modifiers often impact protein localization. Finally, the binding of p53 to an N-terminal region of PARC also suggests an alternative model to PARC-based regulation of p53. The N-terminal region of cullins dictates binding to bridging and substrate specificity proteins, such as SKP1 and F-boxes, and p53 binding to PARC may block the binding of these proteins, inactivating a PARC-based, SCF-like, E3 ubiquitin ligase. Such a model could also explain the apparent discrepancy of a cytoplasmic protein, PARC, binding a predominantly nuclear protein, p53. Under normal conditions an active PARC-based complex could form, degrading specific substrates in isolation from nuclear p53. Upon exposure to genotoxic stresses, the stabilization of p53 allows the cytoplasmic concentration of p53 to rise, acting as an inhibitor of the cytoplasmic PARC complexes. Further work to determine specific substrate adapters for PARC is required to evaluate this model and to examine other potential roles of PARC-p53 complexes.

ACKNOWLEDGMENTS

We thank J. Horner and members of the DFCI Transgenic gene Targeting Core Facility for knockout mouse production; R. DePinho, N. Bardeesy, and A. Aguirre for the pKOII vector, *EIIa-Cre* mice, and general mouse advice; and E. McIntush at Bethyl Laboratories for help in antibody design and production. We also thank the Kazusa DNA Research Institute for KIAA clones, Darrell Borger for the pLB(N)CX T Ag construct, and J. Kasper for sharing unpublished data on CUL7.

J.R.S. was supported by an NSF Graduate Research Fellowship. This work was funded in part by National Cancer Institute grant RO1CA93804.

REFERENCES

1. **Arai, T., J. S. Kasper, J. R. Skaar, S. H. Ali, C. Takahashi, and J. A. DeCaprio.** 2003. Targeted disruption of p185/Cul7 gene results in abnormal vascular morphogenesis. Proc. Natl. Acad. Sci. USA **100:**9855–9860.
2. **Bardeesy, N., M. Sinha, A. F. Hezel, S. Signoretti, N. A. Hathaway, N. E. Sharpless, M. Loda, D. R. Carrasco, and R. A. DePinho.** 2002. Loss of the Lkb1 tumour suppressor provokes intestinal polyposis but resistance to transformation. Nature **419:**162–167.
3. **Cardozo, T., and M. Pagano.** 2004. The SCF ubiquitin ligase: insights into a molecular machine. Nat. Rev. Mol. Cell Biol. **5:**739–751.
4. **Dealy, M. J., K. V. Nguyen, J. Lo, M. Gstaiger, W. Krek, D. Elson, J. Arbeit, E. T. Kipreos, and R. S. Johnson.** 1999. Loss of Cul1 results in early embryonic lethality and dysregulation of cyclin E. Nat. Genet. **23:**245–248.
5. **Deshaies, R. J.** 1999. SCF and Cullin/Ring H2-based ubiquitin ligases. Annu. Rev. Cell Dev. Biol. **15:**435–467.
6. **Dias, D. C., G. Dolios, R. Wang, and Z. Q. Pan.** 2002. CUL7: a DOC domain-containing cullin selectively binds Skp1.Fbx29 to form an SCF-like complex. Proc. Natl. Acad. Sci. USA **99:**16601–16606.
7. **Furukawa, M., Y. J. He, C. Borchers, and Y. Xiong.** 2003. Targeting of protein ubiquitination by BTB-Cullin 3-Roc1 ubiquitin ligases. Nat. Cell Biol. **5:**1001–1007.
8. **Geyer, R., S. Wee, S. Anderson, J. Yates, and D. A. Wolf.** 2003. BTB/POZ domain proteins are putative substrate adaptors for cullin 3 ubiquitin ligases. Mol. Cell **12:**783–790.
9. **Grossberger, R., C. Gieffers, W. Zachariae, A. V. Podtelejnikov, A. Schleiffer, K. Nasmyth, M. Mann, and J. M. Peters.** 1999. Characterization of the DOC1/APC10 subunit of the yeast and the human anaphase-promoting complex. J. Biol. Chem. **274:**14500–14507.
10. **Hershko, A., and A. Ciechanover.** 1998. The ubiquitin system. Annu. Rev. Biochem. **67:**425–479.
11. **Jackson, P. K., and A. G. Eldridge.** 2002. The SCF ubiquitin ligase: an extended look. Mol. Cell **9:**923–925.
12. **Jones, S. N., A. E. Roe, L. A. Donehower, and A. Bradley.** 1995. Rescue of embryonic lethality in Mdm2-deficient mice by absence of p53. Nature **378:** 206–208.
13. **Kikuno, R., T. Nagase, M. Nakayama, H. Koga, N. Okazaki, D. Nakajima, and O. Ohara.** 2004. HUGE: a database for human KIAA proteins, a 2004 update integrating HUGEppi and ROUGE. Nucleic Acids Res. **32**(Database issue)**:**D502–D504.
14. **Kominami, K., I. Ochotorena, and T. Toda.** 1998. Two F-box/WD-repeat proteins Pop1 and Pop2 form hetero- and homo-complexes together with cullin-1 in the fission yeast SCF (Skp1-Cullin-1-F-box) ubiquitin ligase. Genes Cells **3:**721–735.
15. **Lakso, M., J. G. Pichel, J. R. Gorman, B. Sauer, Y. Okamoto, E. Lee, F. W. Alt, and H. Westphal.** 1996. Efficient in vivo manipulation of mouse genomic sequences at the zygote stage. Proc. Natl. Acad. Sci. USA **93:**5860–5865.
16. **Lehman, A. L., Y. Nakatsu, A. Ching, R. T. Bronson, R. J. Oakey, N. Keiper-Hrynko, J. N. Finger, D. Durham-Pierre, D. B. Horton, J. M. Newton, M. F. Lyon, and M. H. Brilliant.** 1998. A very large protein with diverse functional motifs is deficient in rjs (runty, jerky, sterile) mice. Proc. Natl. Acad. Sci. USA **95:**9436–9441.
17. **Li, B., J. C. Ruiz, and K. T. Chun.** 2002. CUL-4A is critical for early embryonic development. Mol. Cell. Biol. **22:**4997–5005.
18. **Mihara, M., S. Erster, A. Zaika, O. Petrenko, T. Chittenden, P. Pancoska, and U. M. Moll.** 2003. p53 has a direct apoptogenic role at the mitochondria. Mol. Cell **11:**577–590.
19. **Montes de Oca Luna, R., D. S. Wagner, and G. Lozano.** 1995. Rescue of early embryonic lethality in mdm2-deficient mice by deletion of p53. Nature **378:**203–206.
20. **Nikolaev, A. Y., M. Li, N. Puskas, J. Qin, and W. Gu.** 2003. Parc: a cytoplasmic anchor for p53. Cell **112:**29–40.
21. **Ohkawa, J., and K. Taira.** 2000. Control of the functional activity of an antisense RNA by a tetracycline-responsive derivative of the human U6 snRNA promoter. Hum. Gene Ther. **11:**577–585.
22. **Pause, A., S. Lee, R. A. Worrell, D. Y. Chen, W. H. Burgess, W. M. Linehan, and R. D. Klausner.** 1997. The von Hippel-Lindau tumor-suppressor gene product forms a stable complex with human CUL-2, a member of the Cdc53 family of proteins. Proc. Natl. Acad. Sci. USA **94:**2156–2161.
23. **Pintard, L., J. H. Willis, A. Willems, J. L. Johnson, M. Srayko, T. Kurz, S. Glaser, P. E. Mains, M. Tyers, B. Bowerman, and M. Peter.** 2003. The BTB protein MEL-26 is a substrate-specific adaptor of the CUL-3 ubiquitin-ligase. Nature **425:**311–316.
24. **Scacheri, P. C., O. Rozenblatt-Rosen, N. J. Caplen, T. G. Wolfsberg, L. Umayam, J. C. Lee, C. M. Hughes, K. S. Shanmugam, A. Bhattacharjee, M. Meyerson, and F. S. Collins.** 2004. Short interfering RNAs can induce unexpected and divergent changes in the levels of untargeted proteins in mammalian cells. Proc. Natl. Acad. Sci. USA **101:**1892–1897.
25. **Shiyanov, P., A. Nag, and P. Raychaudhuri.** 1999. Cullin 4A associates with the UV-damaged DNA-binding protein DDB. J. Biol. Chem. **274:**35309–35312.
26. **Singer, J. D., M. Gurian-West, B. Clurman, and J. M. Roberts.** 1999. Cullin-3 targets cyclin E for ubiquitination and controls S phase in mammalian cells. Genes Dev. **13:**2375–2387.
27. **Staropoli, J. F., C. McDermott, C. Martinat, B. Schulman, E. Demireva, and A. Abeliovich.** 2003. Parkin is a component of an SCF-like ubiquitin ligase complex and protects postmitotic neurons from kainate excitotoxicity. Neuron **37:**735–749.
28. **Suzuki, H., T. Chiba, T. Suzuki, T. Fujita, T. Ikenoue, M. Omata, K. Furuichi, H. Shikama, and K. Tanaka.** 2000. Homodimer of two F-box proteins βTrCP1 or βTrCP2 binds to IκBα for signal-dependent ubiquitination. J. Biol. Chem. **275:**2877–2884.
29. **Tanaka, K., T. Suzuki, T. Chiba, H. Shimura, N. Hattori, and Y. Mizuno.** 2001. Parkin is linked to the ubiquitin pathway. J. Mol. Med. **79:**482–494.
30. **Wang, Y., S. Penfold, X. Tang, N. Hattori, P. Riley, J. W. Harper, J. C. Cross, and M. Tyers.** 1999. Deletion of the Cul1 gene in mice causes arrest in early embryogenesis and accumulation of cyclin E. Curr. Biol. **9:**1191–1194.
31. **Wertz, I. E., K. M. O'Rourke, Z. Zhang, D. Dornan, D. Arnott, R. J. Deshaies, and V. M. Dixit.** 2004. Human De-etiolated-1 regulates c-Jun by assembling a CUL4A ubiquitin ligase. Science **303:**1371–1374.
32. **Wolf, D. A., F. McKeon, and P. K. Jackson.** 1999. F-box/WD-repeat proteins pop1p and Sud1p/Pop2p form complexes that bind and direct the proteolysis of cdc18p. Curr. Biol. **9:**373–376.
33. **Xu, L., Y. Wei, J. Reboul, P. Vaglio, T. H. Shin, M. Vidal, S. J. Elledge, and J. W. Harper.** 2003. BTB proteins are substrate-specific adaptors in an SCF-like modular ubiquitin ligase containing CUL-3. Nature **425:**316–321.
34. **Yu, X., Y. Yu, B. Liu, K. Luo, W. Kong, P. Mao, and X. F. Yu.** 2003. Induction of APOBEC3G ubiquitination and degradation by an HIV-1 Vif-Cul5-SCF complex. Science **302:**1056–1060.
35. **Zhu, Q., J. Yao, G. Wani, J. Chen, Q. E. Wang, and A. A. Wani.** 2004. The ubiquitin-proteasome pathway is required for the function of the viral VP16 transcriptional activation domain. FEBS Lett. **556:**19–25.